Clays and Clay Minerals, Vol. 44, No. 2, 191–196, 1996.

WHY DOES HALLOYSITE ROLL?—A NEW MODEL

BALBIR SINGH

Centre for Microscopy and Microanalysis, The University of Queensland
Brisbane, Qld. 4072, Australia

Abstract—A model is presented to explain why tubular halloysite rolls in preference to tetrahedral rotation to correct misfit of the octahedral and tetrahedral sheets. It is shown that the rolling mechanism operates as it encounters significantly less resistance from Si–Si repulsion in comparison to tetrahedral rotation to correct the same amount of misfit. The model explains the observed and experimental rolling of planar kaolinites to form tubular halloysite upon hydration and exfoliation.

Key Words—Coulomb repulsion, Kaolinite, Rolling, Tetrahedral rotation, Tubular Halloysite.

INTRODUCTION

Although a large volume of literature has been devoted to the study of various aspects of halloysite, a number of major issues related to its structure and morphology remain unresolved (Giese 1988). Bailey (1989) critically reviewed the current literature on structure, morphology and chemical composition of halloysite, and highlighted the clear gaps in our understanding of this common clay mineral. As illustrated by Bailey (1989), the major questions that remain to be answered are: (1) why does halloysite roll; (2) why does it always roll its a-axis in preference to the b-axis; and (3) why does halloysite have interlayer water? This paper briefly discusses the limitations of current theories explaining why halloysite rolls and then develops a new model to explain this phenomenon. A complete discussion on the limitations of current theories is given by Bailey (1989). The model presented here is supported by reference to published and experimental data (Singh and Mackinnon personal communication), and well accepted crystallochemical principles.

REVIEW OF CURRENT THEORIES

Bates et al. (1950) proposed that the 1:1 layer of halloysite rolls, with the tetrahedral sheet on the outside of the curve, in order to minimize the misfit of the larger tetrahedral and smaller octahedral sheets. Assuming hexagonal symmetry and an ideal hexagonal shape, the lateral dimensions of a tetrahedral sheet can be calculated from the equation:

$$b = (4\sqrt{2})(T - -O) \quad [1]$$

For a Si-tetrahedral sheet with a Si–O bond length of 1.62 Å (Bailey 1989), the b dimension equals 9.164 Å and a = 5.02 Å. These lateral dimensions of the tetrahedral sheet are significantly larger than those of the Al-dioctahedral sheet which has b = 8.655 Å and a = 5.066 Å as observed for gibbsite. Bates et al. (1950) showed that the calculated diameter of the tubes match well with the observed minimum internal diameter of the halloysite tubes (Figure 1).

Radoslovich (1963b) demonstrated that the misfit of lateral dimensions of 1:1 and 2:1 structures can be readily corrected by rotation of the adjacent tetrahedra in opposite directions. This mechanism causes every basal oxygen, Si and apical oxygen atom of the tetrahedral sheet to move closer to the ring center, thereby reducing its lateral dimensions and adopting a ditrigonal ring configuration (Figure 2). Radoslovich (1963b) argued that the dimensions of the tetrahedral sheet of halloysite can be effectively reduced by tetrahedral rotation as in the case of kaolinite, but halloysite rolls due to contraction of the OH–OH bonds in the surface OH plane. According to Radoslovich (1963b), the contraction of the outer OH plane in this fashion causes the octahedral sheet and the attached tetrahedral sheet to curl.

Bailey (1989) cited the occurrence of platey halloysites and demonstrated that the platey morphology of these specimens is a result of elimination of the misfit due to substitution of the larger Fe^{3+} cation in the octahedral sheet. According to the theory of Radoslovich (1963b), the Fe-rich halloysites should have rolled forms which is not the case. Thus, the absence of rolling in Fe-rich halloysites demonstrates that the OH-OH contraction is not an effective force in halloysite rolling.

The occurrence of Fe-rich platey halloysite supports the theory of Bates et al. (1950), but it is still not clear why tetrahedral rotation does not take place in tubular halloysites. In an attempt to answer this question, Bailey (1989) hypothesized that all forms of halloysite have a net negative charge arising from the substitution of Si^{4+} by Al^{3+} or Fe^{3+} that provides a driving force for the introduction of water and hydrated cations into the interlayer space. Bailey (1989) further proposed that the interlayer water and cations are located in the hexagonal cavities at the same z coordinate as basal oxygen, and block the rotation of tetrahedra, forcing the layers to roll in order to correct the

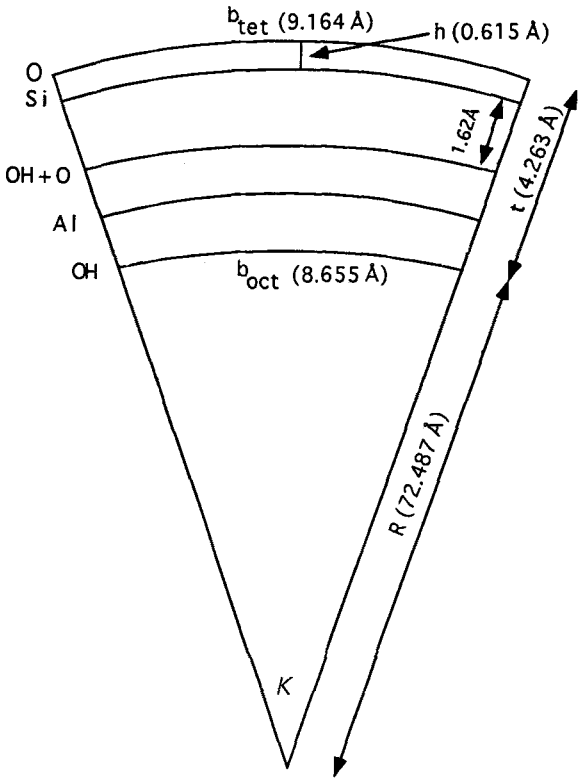

Figure 1. A schematic diagram showing rolling of tetrahedral and octahedral sheet to correct lateral misfit (Bates et al. 1950).

misfit. Thus, according to Bailey (1989) interlayer water plays a dual role in rolling of halloysite: (1) to block the tetrahedral rotation and (2) to relax the interlayer hydrogen bonding.

The model by Bailey (1989) requires all types of halloysites to have tetrahedral substitution. Many recent studies have shown that perfectly tubular halloysites do not have a negative charge as indicated by their low cation exchange capacity and an ideal chemical composition (Tazaki 1982; Banfield and Eggleton 1990; Singh and Gilkes 1991, 1992). More recently, Newman et al. (1994) investigated a range of six well-characterized halloysites and Georgia kaolinite using Al-27 solid-state NMR spectroscopy in an attempt to find evidence for Al (IV) as suggested by Bailey (1989). They concluded that interlayer water cannot be attributed to substitution of Si by Al as the contents of Al (IV) for both halloysites and Georgia kaolinite were less than 1%. Therefore, it appears that interlayer water in halloysite is driven into the interlayer due to its activity and/or structural disorder, and may not be specifically adsorbed on the tetrahedral side of the interlayer space. Many clay minerals such as smectites and artificially hydrated kaolinite (Costanzo and Giese 1985) can accommodate water in the interlayer without affecting tetrahedral rotation which is common in

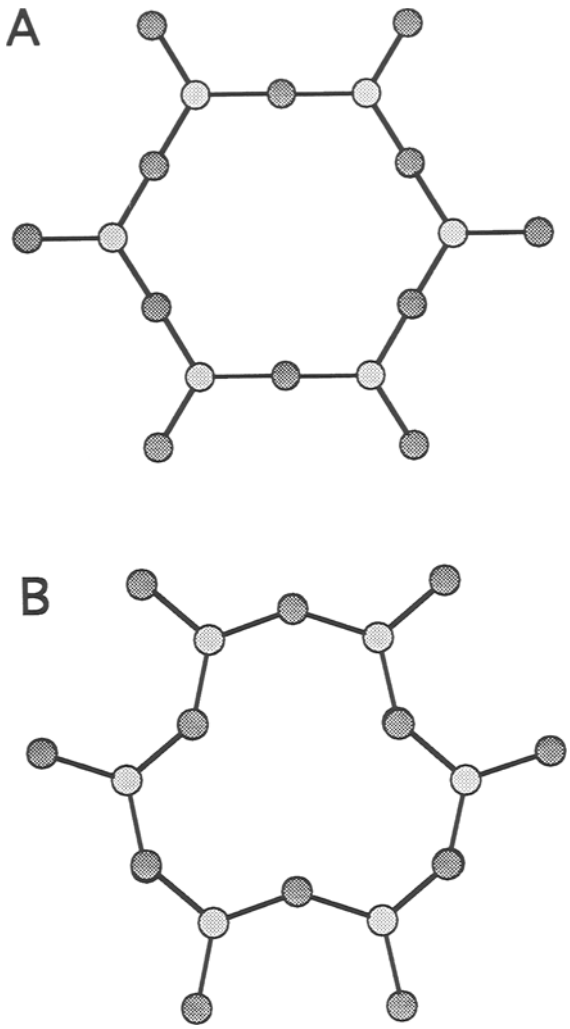

Figure 2. A schematic diagram of a unit of a hexagonal (A) and ditrigonal tetrahedral sheet (B). Rotation of tetrahedra about their apices in opposite directions reduces the lateral dimension of the tetrahedral sheet, and changes its configuration from hexagonal to ditrigonal.

these minerals. Thus, there is no clear evidence to support the hypothesis that tetrahedral rotation in halloysite may be blocked by interlayer water. However, the role of interlayer water to disrupt hydrogen bonding across the interlayer is well accepted (Costanzo and Giese 1985).

A NEW MODEL

Atomic scale stresses due to a larger tetrahedral sheet and a smaller octahedral sheet in a 1:1 layer originate at two planes: (1) the basal oxygen plane of the tetrahedral sheet and (2) the inner OH, O plane (Figure 3). The stress of type 1 is sufficiently relieved for hydrated halloysite by the presence of water molecules and separation of the layers by a distance of

https://doi.org/10.1346/CCMN.1996.0440204 Published online by Cambridge University Press

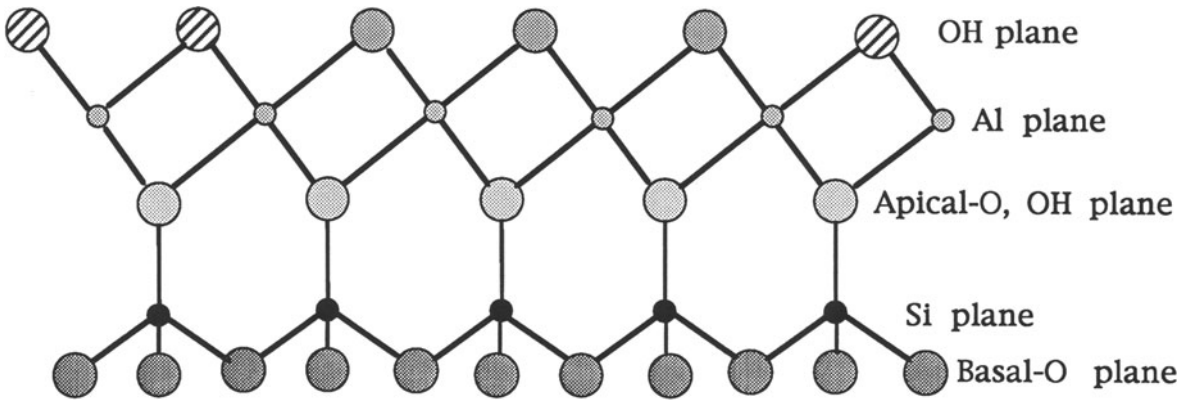

Figure 3. A schematic diagram showing atomic planes in a 1:1 layer. In halloysite, stress due to misfit of the sheets originates from the middle of the 1:1 layer.

5.74 Å (Bates et al. 1950; Bailey 1989). However, the stress of type 2 is not affected by hydration of the interlayer space as it lies in the middle of the 1:1 layer. The apical oxygens of the tetrahedral sheet lie in the same plane as OH and are shared by the octahedral cations. Since the tetrahedral sheet is larger than the octahedral sheet, the Al–O bonds, which bind the two sheets, are stretched, and their tendency to attain ideal bond lengths forces the contraction of the apical oxygen plane. Thus, the stress due to misfit of the tetrahedral and octahedral sheet in the hydrated 1:1 layer originates from the middle of the 1:1 layer, and is then transmitted through Si–O covalent bonds to the Si plane and the basal oxygen plane. The intensity of this stress is attenuated by the angular flexibility of the Si–O bonds as it is transmitted from the central O, OH plane to the Si and then to the basal oxygen plane. Thus, for a hydrated 1:1 layer the only compelling requirement is to correct the misfit between the apical oxygen plane and the inner OH plane so that they can merge into a single plane (the O–OH plane). The dimensions of the Si and basal oxygen plane of the tetrahedral sheet are affected only as a consequence of contraction of the apical oxygen plane.

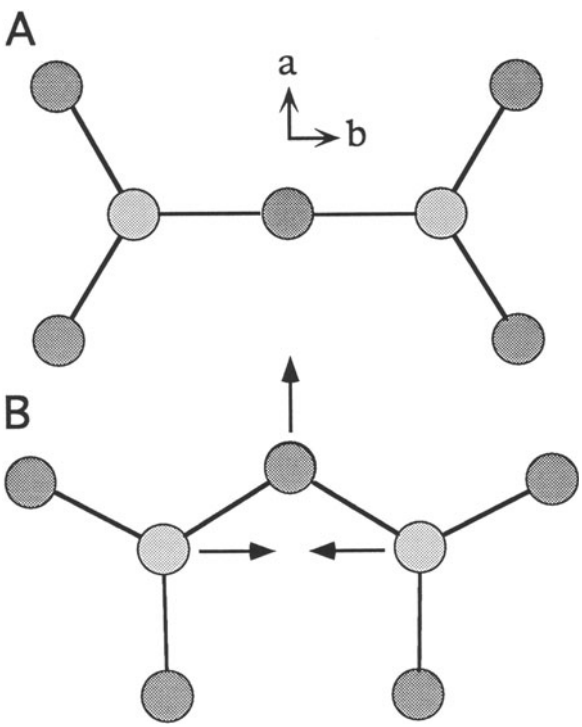

Figure 4. A schematic diagram showing two adjacent tetrahedra for a hexagonal (A) and a ditrigonal (B) tetrahedral sheet. The distances between adjacent apical oxygens in the ditrigonal tetrahedral sheet have been reduced by tetrahedral rotation in the opposite directions.

The misfit between the apical oxygen plane and the inner OH plane can be corrected by either (1) tetrahedral rotation (Figures 2 and 4) or (2) by rolling of the 1:1 layer (Figures 1 and 5). Tetrahedral rotation shrinks the distances to an equal amount for all of the three atomic planes in the tetrahedral sheet, that is basal oxygen, Si and apical oxygen plane, and in all the directions in the ab plane (Figure 2). Whereas the rolling mechanism contracts the distances only for the rolled axis, and the contraction is greater for the apical oxygen plane, due to being inside the curvature relative to the Si and the basal oxygen plane. As discussed earlier, the only compelling requirement for the hydrated halloysite is to have equal dimensions of the apical oxygen plane and the inner OH plane. Any associated contraction of the Si or basal oxygen plane is unnecessary. The tetrahedral rotation contracts the Si and basal oxygen plane to the same extent as the apical oxygen and consequently encounters greater resistance from the cation–cation and anion–anion repulsion in these planes. The most economical way to correct this misfit for a given direction is by rolling as this mechanism causes minimum contraction of the Si and basal oxygen plane (Figure 5).

https://doi.org/10.1346/CCMN.1996.0440204 Published online by Cambridge University Press

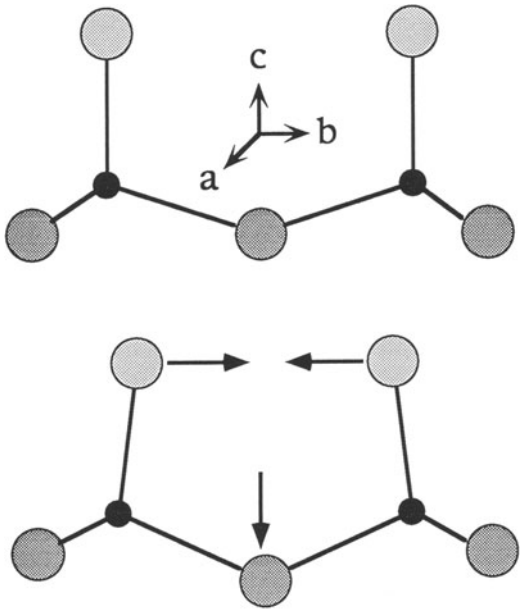

Figure 5. A schematic diagram showing two adjacent tetrahedra for a planar (A) and curved tetrahedral sheet (B). The distance of apical oxygens in the curved sheet have been reduced by decreasing the Si-O-Si angle.

The shape and dimensions of the tetrahedral sheet are determined by an equilibrium between three types of forces, namely (1) cation–cation repulsion in the Si plane; (2) anion–anion repulsion in the basal apical oxygen plane; and (3) cation–anion bonds. An unconstrained tetrahedral sheet has a fully expanded hexagon in order to minimize the Si–Si Coulomb repulsion. Any external force that decreases the distance between cations will be opposed by cation–cation Coulomb repulsion (Bailey 1980).

Cation–cation repulsion plays a major role in the determination of cell dimensions, stability and stacking of layer silicates. For example, Coulomb repulsion between tetrahedral and octahedral cations is considered a significant instability factor in the Group A layer sequence of kaolinite, halloysite and dickite, and accounts for the rare occurrence of a Group A sequence in trioctahedral 1:1 minerals. The effectiveness of cation-cation repulsion is well recognized for the octahedral sheet where adjacent octahedra share edges (Radoslovich 1963a). The Si atoms in tetrahedra are shielded by oxygen atoms, but not completely. In a planar tetrahedral sheet, the Si atom plane lies 0.615 Å (Bates et al. 1950) above the basal oxygen plane. The oxygen atoms physically cover the Si atoms due to their larger atomic radii, but may not completely offset the Si–Si electrostatic repulsion.

For quantitative comparison of the rolling and rotation mechanism, the Si–Si repulsion encountered by either mechanism to correct a given amount of misfit can be determined using Coulomb's law:

$$F = \frac{(q \cdot q')}{r^2} \quad [2]$$

Where F is the repulsion force, q and q′ are the charges in electrostatic units and r is the distance between charges. The relative increase in repulsion for a ditrigonal and curved hexagonal sheet can be calculated from the relation:

$$F_{rel} = (r_h/r)^2 \quad [3]$$

Where F_{rel} is the relative repulsion, r_h is the Si–Si distance in a planar hexagonal tetrahedral sheet and r is the Si–Si distance in a curved or ditrigonal tetrahedral sheet. The value of r for hexagonal planar and ditrigonal sheets can be calculated from the b dimension using the relation:

$$r = \frac{b}{3} \quad [4]$$

The b dimensions of a hexagonal planar tetrahedral sheet and the octahedral sheet are given above, and the b dimension on a ditrigonal tetrahedral sheet equals that of an octahedral sheet.

For calculation of r for a curved tetrahedral sheet, we need to determine to what extent the Si plane will contract relative to the basal oxygen plane.

It can be seen from Figure 1 that:

$$b_{tet} = k \cdot (R + t) \quad [5]$$

$$b_{oct} = k \cdot R \quad [6]$$

Where b_{tet} is the b dimension of a planar tetrahedral sheet and b_{oct} is the b dimension of an octahedral sheet. R is the inner radius of curvature of the 1:1 layer, t is the combined thickness of the tetrahedral and octahedral sheets and k is the angle of curvature in radians.

From Equations [5] and [6]:

$$k = (b_{tet} - b_{oct})/t \quad [7]$$

Substituting k in Equation [6]:

$$R = b_{oct} \frac{t}{(b_{tet} - b_{oct})} \quad [8]$$

$$R_{Si} = (R + t - h) \quad [9]$$

where R_{Si} is the radius for Si atoms and h is the distance between Si atoms and the outer periphery of the tube with a value of 0.615 Å (Bates et al. 1950). The contraction factor for Si, C_{Si}, is given by the equation:

$$C_{Si} = \frac{R_{Si}}{(R + t)} \quad [10]$$

$$r_{cur} = r_h \cdot C_{Si} \quad [11]$$

The Si–Si distances for hexagonal, ditrigonal and curved tetrahedral sheets have been calculated using the above procedure. The relative repulsion encountered by the two mechanisms is then calculated using

https://doi.org/10.1346/CCMN.1996.0440204 Published online by Cambridge University Press

Table 1. Percent increase in Si–Si repulsion encountered by adjacent Si atoms in curved hexagonal (those of curved 1:1 layer) and planar ditrigonal tetrahedral sheets. The relative repulsion is calculated using Equation 3.

Type of sheet	Si–Si distance	Relative repulsion	% increase
Planar hexagonal	3.0546 Å	1	0
Curved hexagonal	3.041 Å	1.01	1
Planar ditrigonal	2.885 Å	1.12	12

Equation 3. The calculated data show that the rolling mechanism results in only a 1% increase in Coulomb repulsion between adjacent Si atoms (Table 1). Whereas the tetrahedral rotation encounters 12 times greater repulsion in comparison to the rolling mechanism for correction of the same amount of misfit.

The above comparison of tetrahedral rotation and rolling mechanism is valid only for a hydrated 1:1 structure. In the case of non-hydrated 1:1 structures, hydrogen bonding is a dominant force which requires the structure to correct the alignment between basal oxygens and outer OH groups. It is well-known that tetrahedral rotation results in shorter hydrogen bonds between basal oxygens and OH groups across the interlayer space (Bailey 1988). Therefore, in the case of non-hydrated 1:1 structures, the tendency to make shorter hydrogen bonds between the basal oxygen and outer OH plane provides an additional driving force for tetrahedral rotation. Thus, tetrahedral rotation corrects the misfit on both sides of the tetrahedral sheet of a non-hydrated 1:1 structure, a result which cannot be accomplished by a rolling mechanism.

In both mechanisms, the dimensions of the apical oxygen plane are reduced by modifying the Si-O-Si bond angles in the basal oxygen plane (Figures 4 and 5). The difference between the two mechanisms can be understood by visualizing the translation of basal oxygen in relation to the Si atoms. In the case of tetrahedral rotation, the basal oxygen translates in the lateral direction, whereas in the case of a rolling mechanism, the basal oxygens translate in the z direction toward the interlayer space. Since the Si-O-Si bond lengths are kept constant, the Si atoms move closer to each other. Although the two mechanisms produce greatly different morphologies, that is tubes and plates, the fundamental difference between them is simply the direction in which the basal oxygen translates.

The basal oxygen can also translate in a direction between the z and lateral directions. In other words, misfit can be corrected by a combination of a rolling mechanism and tetrahedral rotation. Presumably, the rolling mechanism operates first to a maximum possible extent as it is more efficient, and then the remainder of the misfit is corrected by tetrahedral rotation. The rolling mechanism corrects the misfit completely only when the radius of curvature is about 98 Å. This radius of curvature is consistent with the smallest inner diameter observed in halloysite tubes of varying origins. The radius of halloysite tubes commonly range between 0.05 and 0.5 μm (Singh and Gilkes 1992). Therefore, only a few layers in a tube of average size can have complete correction of the misfit by the rolling mechanism. It appears that for layers with a radius greater than 98 Å, the residual misfit is corrected by tetrahedral rotation as described above, that is the basal oxygen atoms translate in both the z and lateral directions.

The octahedral sheet probably provides only negligible resistance to rolling. The cations are located in the middle of the sheet so that the cation–cation distance remains unchanged as the sheet is curved/rolled.

Supporting Evidence

The theoretical analysis given above shows that for a hydrated 1:1 layer, rolling is a more efficient mechanism in comparison to tetrahedral rotation for correction of the lateral misfit. It also shows that the fundamental difference between the two mechanisms is rather small thus the 1:1 structure can gradually shift from one mechanism to the other as the state of hydration changes. Therefore, one would expect platey kaolinite to roll once interlayer hydrogen bonding has been weakened by hydration. Singh and Mackinnon (personal communication) have indeed found this in an experiment conducted to test this hypothesis. Singh and Mackinnon hydrated Georgia kaolinite (KGa-1) using potassium acetate as an entraining agent. Upon hydration, the plates of Georgia kaolinite roll along major crystallographic directions to produce tubes that exhibit morphology and electron diffraction characteristics identical to those of proper halloysite tubes.

Recent TEM investigations of natural samples have also indicated that platey kaolinite may roll or curve to produce halloysite tubes (Singh and Gilkes 1992; Robertson and Eggleton 1991). In the kaolin material described by Singh and Gilkes (1992), kaolinite pseudomorphs after mica fractured and rolled to form an array of oriented halloysite tubes. Similarly, Robertson and Eggleton (1991) observed that kaolinite plates formed by weathering of muscovite fanned (exfoliated at edges) and folded to form tubes. Figures 7 and 13 of Singh and Gilkes (1992) and Figure 4 of Robertson and Eggleton (1991) provide strong direct evidence that platey kaolinite transformed in the solid state to tubular halloysite. Presumably, prior to folding or rolling, the misfit in the planar forms of these materials was corrected by tetrahedral rotation as in the case of kaolinite, and the structure switched to the rolling mechanism after hydration and/or removal of physical constraints to exfoliation and rolling (Robertson and Eggleton 1991; Singh and Gilkes 1992). However, the reasons for hydration of kaolinite in a natural environment are not clear.

Similarly, the 1:1 structure can also switch from the rolling mechanism to tetrahedral rotation. Upon dehydration of the hydrated 1:1 structure, the interlayer hydrogen bonding becomes a dominant force and favors rotation of tetrahedra in order to shorten hydrogen bonds (Bailey 1988). Churchman and Gilkes (1989) observed unrolled tubes (laths) in the surface horizons of highly weathered lateritic profiles. Unlike dehydrated halloysites, these kaolins showed intercalation properties similar to those of kaolinite, indicating that hydrogen bonding in these materials is as strong as in kaolinite. On the basis of intercalation properties and lath-like morphology, Churchman and Gilkes (1989) classified these materials as kaolinites produced by prolonged dehydration of tubular halloysite. Apparently, as a result of prolonged dehydration, the hydrogen bonding between the layers gradually became stronger, and the structure gradually shifted from a rolling mechanism to tetrahedral rotation, causing the tubes to produce laths by unrolling. Thus, the transformation of tubular halloysite to platey kaolinite on dehydration is the reverse case of transformation of platey kaolinite to tubular halloysite on hydration.

SUMMARY

The theories of Radoslovich (1963b) and Bailey (1989) appear to assume that tetrahedral rotation is a "freely" available mechanism to reduce the lateral dimensions of the tetrahedral sheet. The author considers that the tetrahedral rotation and rolling mechanisms are both resisted by Si–Si Coulomb repulsion in the Si plane. The rolling mechanism operates in hydrated halloysite in preference to tetrahedral rotation because the least resistance is offered by Si–Si repulsion. The 1:1 kaolin structure can switch from tetrahedral rotation to a rolling mechanism and vice versa in response to changes in the state of hydration provided there are no other physical constraints.

ACKNOWLEDGMENTS

The author gratefully acknowledges encouragement and critical reviews provided by I. D. R. Mackinnon, S. W. Bailey and Balwant Singh.

REFERENCES

Bailey SW. 1980. Kaolin minerals. In:Brindley GW, Brown G, editors. Crystal structures of clay minerals and their X-ray identification. London:Mineralogical Society. 1–123.

Bailey SW. 1988. Polytypism of 1:1 layer silicate. In: Bailey SW, editor. Hydrous phyllosilicates (exclusive of mica). MSA Reviews in Mineralogy 19:9–27.

Bailey SW. 1989. Halloysite—A critical assessment. In: Farmer VC, Tardy Y, editors. Proc. Int. Clay Conf. Strasbourg, France. Sci Geol Mem 86:89–98.

Banfield JF, Eggleton RA. 1990. Analytical transmission electron microscope studies of plagioclase, muscovite, and K-feldspar weathering. Clays & Clay Miner 38:77–89.

Bates TF, Hildebrand FA, Swineford A. 1950. Morphology and structure of endellite and halloysite. Am Mineral 6: 237–248.

Churchman GJ, Gilkes RJ. 1989. Recognition of intermediates in the possible transformation of halloysite to kaolinite in weathering profiles. Clay Miner 24:579–590.

Costanzo PM, Giese Jr RF. 1985. Dehydration of synthetic hydrated kaolinite: a model for dehydration of halloysite (10Å). Clays & Clay Miner 33:415–423.

Giese Jr RF. 1988. Kaolin minerals: Structures and stablities. In:Bailey SW, editor. Hydrous phyllosilicates (exclusive of micas). MSA Reviews in Mineralogy 19:29–66.

Newman R, Childs C, Churchman J. 1994. Aluminium coordination and structural disorder in halloysite and kaolinite by ^{27}Al NMR spectroscopy. Clays & Clay Miner 29:305–312.

Radoslovich EW. 1963a. The cell dimensions and symmetry of layer-lattice silicate. IV. Inter atomic forces. Am Mineral 48:76–99.

Radoslovich EW. 1963b. The cell dimensions and symmetry of layer-lattice silicate. VI. Serpentine and kaolin morphology. Am Mineral 48:368–378.

Robertson IDM, Eggleton RA. 1991. Weathering of granitic muscovite to kaolinite and halloysite and of plagioclase-derived kaolinite to halloysite. Clays & Clay Miner 39: 113–126.

Singh Balbir, Gilkes RJ. 1991. Weathering of chromian muscovite to kaolinite. Clays & Clay Miner 39:571–579.

Singh Balbir, Gilkes RJ. 1992. An electron-optical investigation of the alteration of kaolinite to halloysite. Clays & Clay Miner 40:212–229.

Singh Balbir, Mackinnon IDR. personal communication. Center for Microscopy and Microanalysis. The University of Queensland. Brisbane, Qld. 4072, Australia.

Tazaki K. 1982. Analytical electron microscopic studies of halloysite formation- morphology and composition of halloysite. Proc. 7th Int. Clay Conf., Italy 573–584.

(Received 10 August 1994; accepted 14 July 1995; Ms. 2560)